Noninvasive optical cytochrome c oxidase redox state measurements using diffuse optical spectroscopy

Jangwoen Lee,[a,*] Jae G. Kim,[a,b] Sari B. Mahon,[a] David Mukai,[a] David Yoon,[a] Gerry R. Boss,[c] Steven E. Patterson,[d] Gary Rockwood,[e] Gary Isom,[f] and Matthew Brenner[a,g,*]

[a]University of California Irvine, Beckman Laser Institute and Medical Clinic, 1002 Health Sciences Road East, Irvine, California 92612
[b]Gwangju Institute of Science and Technology, School of Information and Communications, Department of Medical System Engineering, 123 Cheomdan-gwagiro, Buk-gu, Gwangju 500-712, Republic of Korea
[c]University of California San Diego, Department of Medicine, 9500 Gilman Dr., La Jolla, California 92093
[d]University of Minnesota, Department of Pharmacology, 516 Delaware Street SE, Minneapolis, Minnesota 55455
[e]US Army Medical Research Institute of Chemical Defense, Aberdeen Proving Ground, Maryland 21010
[f]Purdue University, Department of Medicinal Chemistry and Molecular Pharmacology, 575 Stadium Mall Drive, West Lafayette, Indiana 47907
[g]University of California Irvine Medical Center, Department of Pulmonary and Critical Care, 333 West City Boulevard, Suite 400, Orange, California 92868

Abstract. A major need exists for methods to assess organ oxidative metabolic states *in vivo*. By contrasting the responses to cyanide (CN) poisoning versus hemorrhage in animal models, we demonstrate that diffuse optical spectroscopy (DOS) can detect cytochrome c oxidase (CcO) redox states. Intermittent decreases in inspired O_2 from 100% to 21% were applied before, during, and after CN poisoning, hemorrhage, and resuscitation in rabbits. Continuous DOS measurements of total hemoglobin, oxyhemoglobin, deoxyhemoglobin, and oxidized and reduced CcO from muscle were obtained. Rabbit hemorrhage was accomplished with stepwise removal of blood, followed by blood resuscitation. CN treated rabbits received 0.166 mg/ min NaCN infusion. During hemorrhage, CcO redox state became reduced concurrently with decreases in oxyhemoglobin, resulting from reduced tissue oxygen delivery and hypoxia. In contrast, during CN infusion, CcO redox state decreased while oxyhemoglobin concentration increased due to CN binding and reduction of CcO with resultant inhibition of the electron transport chain. Spectral absorption similarities between hemoglobin and CcO make noninvasive spectroscopic distinction of CcO redox states difficult. By contrasting physiological perturbations of CN poisoning versus hemorrhage, we demonstrate that DOS measured CcO redox state changes are decoupled from hemoglobin concentration measurement changes.
[DOI: 10.1117/1.JBO.19.5.055001]

Keywords: diffuse optical spectroscopy; cytochrome c oxidase; physiological perturbation; cyanide poisoning; hemorrhage.

Paper 130482RR received Jul. 10, 2013; revised manuscript received Mar. 1, 2014; accepted for publication Mar. 7, 2014; published online May 1, 2014.

1 Introduction

Cyanide (CN) based derivatives have been used for centuries as poisons and chemical weapons.[1,2] CN continues to pose a major potential chemical threat to civilians and military personnel.[2,3] The mechanisms of CN toxicity are complex.[4,5] A main target of CN toxicity is CN impairment of the ability of tissues to utilize oxygen through inhibition of cytochrome c oxidase (CcO).[3] CcO is the terminal oxidase of the mitochondrial respiratory chain and transfers electrons from ferrocytochrome c to molecular oxygen.[6] CcO is involved in >95% of the oxygen consumption in the body and is essential for the efficient generation of cellular ATP.[7] CN has a high binding affinity for active sites on CcO. Progressive cytotoxic tissue hypoxia develops quickly after CN binding and immediate intervention is necessary to prevent toxicity and death.[8] Thus, the need for rapid identification of patients exposed to CN and ability to continuously monitor the response to treatment in field or hospital settings is critical. This need is compounded by the potentially large number of people with significant risks of severe injury from intentional or accidental mass casualty exposure events.

Moreover, the ability to measure CcO redox state *in vivo* is an important unmet need in clinical and research medicine. CcO redox status is a direct reflection of adequacy of tissue perfusion, oxygenation, and cellular metabolic status at the mitochondrial level. Investigators have sought accurate methods to noninvasively monitor the CcO redox status to determine whether the tissue and organs are in healthy, stressed, or diseased states.[9–19] In order to guide diagnostics, therapeutics, and resuscitation, noninvasive and continuous measurements of CcO redox state would be optimal.

Since CcO contains four redox active metal centers (two heme and copper groups respectively) and these metal centers give rise to absorption bands in ultraviolet, visible, and near-infrared (NIR) regions, photonics based technologies such as near-infrared spectroscopy (NIRS) have utilized the unique absorption spectra of the oxidized and reduced states of CcO in order to attempt to determine the physiological oxygenation status of tissue and organs *in vivo*.[9,16,20]

This change of absorption spectra associated with CcO redox state changes presents a potential noninvasive diagnostic opportunity for diffuse optical spectroscopy (DOS).[21–23] DOS combines multifrequency frequency domain photon migration (FDPM) with time-independent NIRS to quantitatively measure bulk tissue absorption and scattering spectra. DOS has been

*Address for correspondence to: Jangwoen Lee, E-mail: jangwl@uci.edu; Matthew Brenner, E-mail mbrenner@uci.edu

applied to various clinical situations including breast cancer monitoring and clinical care monitoring. Especially in clinical care monitoring, it has been successfully employed in monitoring hemorrhage and fluid resuscitation,[24,25] the formation and treatment of methemoglobinemia,[26] and CN poisoning by quantifying the tissue concentrations of hemoglobin species and relevant chromophores.[27,28]

In addition, we have used DOS measurements of tissue hemoglobin concentrations during CN poisoning and treatment phases in order to determine the efficacy of various CN antidotes.[29–31] Although DOS and continuous wave NIRS measurements have proven valuable to determine the effectiveness of CN antidotes, we have relied primarily on the kinetics of oxy- and deoxyhemoglobin concentration changes such as decay time constants after the antidote injection. However, the changes in tissue hemoglobin concentrations at the onset of CN poisoning also includes other confounding factors such as cardiovascular changes and severe metabolic acidosis which, in turn, can affect tissue hemoglobin concentrations. Therefore, the assessment of CcO redox states would potentially show cellular metabolic status during CN poisoning and the effects of CN antidotes more directly.

CN has been used previously in NIRS measurement of CcO *in vivo* as a CcO and electron transport chain inhibitor.[13,14,32] CN poisoning presents a unique situation with regard to CcO and hemoglobin oxygenation. During CN poisoning, tissues are unable to extract oxygen from hemoglobin and optical measures of tissue hemoglobin saturation increase,[27,29–31] while principal electron transport chain cytochromes are reduced.[14,33] As the four metal centers in the CcO undergo changes in redox state during CN poisoning, they change absorption spectra. As CN binds to Cyt a3 of CcO, it prevents oxygen reduction of the electrons leaving CuA.[34] As a result, the CuA center, which accounts for the majority of the NIR absorption signal of CcO), becomes reduced.[32,35,36]

Unfortunately, noninvasive spectroscopic monitoring of CcO redox information *in vivo* has been limited by (i) a lack of clearly valid gold standard cytochrome oxidase measures for comparison and (ii) major concerns regarding optical interference from "cross talk" from dominant hemoglobin and myoglobin absorption signals in tissues.[16,37]

The objective of this study is to provide evidence for the validity of *in vivo* measurement of cytochrome oxidase redox state changes during CN poisoning with DOS in peripheral muscle. We report a series of experiments designed to noninvasively assess CcO redox states *in vivo* and demonstrate independence from hemoglobin (or myoglobin) "optical crosstalk" using DOS. These studies involve a combination of CN poisoning, hemorrhage, and alterations in inspired oxygen concentration in animal models undergoing continuous DOS monitoring.

Under most clinical conditions, CcO redox state changes parallel to those of hemoglobin oxygen delivery and supply to the tissues. Therefore, it has not been possible to convincingly demonstrate that optical signals that are presumed to be generated from CcO redox state changes are independent from changes in hemoglobin (or myoglobin in muscle) redox state measurements.[14] For example, during hemorrhage, reduction in tissue hemoglobin-based oxygen delivery, increase in tissue oxygen extraction coefficients, and decreased tissue hemoglobin (and/or myoglobin) oxygenation are associated with concurrent reduction in tissue cytochrome oxidation state.[14] This is particularly important, since hemoglobin absorption in the NIR region has been reported to be approximately an order of magnitude higher than the cytochrome absorption signals.[14,37] A similar parallel change in redox states for hemoglobin and CcO occurs during reduction in inspired oxygen, and other hypoxemic or hypoperfusion states. Thus, it has not been possible in these scenarios to clearly separate photonics-based measured changes in CcO from hemoglobin redox state changes with certainty.

CN poisoning presents a unique situation with regard to CcO and hemoglobin oxygenation. During CN poisoning, tissues are unable to extract oxygen from hemoglobin and tissue hemoglobin saturations increase, while principal electron transport chain cytochromes are reduced. Thus, during CN poisoning, hemoglobin (and/or myoglobin) oxygenation states change in the opposite direction of CcO redox state.[14]

Therefore, by contrasting the differences of DOS based optical CcO redox state between hemorrhage-induced CcO and hemoglobin redox signals against CN-induced changes, together with the response to varying inhaled oxygen concentrations, it is possible to demonstrate uncoupling of these optical signals as demonstrated in this study.

2 Materials and Methods

The methods for CN induction and DOS monitoring in rabbits have been previously described[27] and are summarized here.

2.1 *Rabbit Studies*

The protocol was reviewed and approved by the University of California Irvine (UCI) Institutional Animal Care and Use Committee (IACUC). Fourteen pathogen-free New Zealand white rabbits (Western Oregon Rabbit Supply, Philomath, Oregon), weighing 3.76 ± 0.03 kg (mean $\pm$ standard error of mean) were used in this study. Animals were anesthetized with an intramuscular injection of Ketamine HCl 50 mg/kg (Ketaject, Phoenix Pharmaceutical Inc., St. Joseph, Michigan) and Xylazine 5 mg/kg (Anased, Lloyed Laboratories, Shenandoah, Iowa). After the injection, a catheter was placed in the animal's marginal ear vein to administer continuous intravenous anesthesia with Ketamine/Xylazine. Animals were mechanically ventilated (dual phase control respirator, model 32A4BEPM-5R, Harvard Apparatus, Chicago, Illinois) at a rate of 20 respirations per min, a tidal volume of 50 cc, and inspired O_2 concentration of 100%. A pulse oximeter (Biox 3700 Pulse Oximeter, Ohmeda, Boulder, Colorado) with a probe was placed on the tongue, to measure SpO_2 and heart rate.

Rabbits were anesthetized, intubated, ventilated, and monitored with continuous DOS measurements of oxyhemoglobin, deoxyhemoglobin, lipid, water content measurements as well as CcO redox states. Measurements were obtained from the DOS probe placed over the right thigh muscle region. Monitoring of blood pressure and blood gas sampling were accomplished through femoral arterial and venous lines. Respiratory challenges, with intermittent decreases (5 min) in inspired O_2 from 100% to 21%, were applied before, during hemorrhage and resuscitation (in hemorrhage study animals), as well as before, during, and after CN infusion (in CN study animals).

2.2 *Control Animals*

Control animals ($n = 5$) received neither CN nor hemorrhage, but were monitored throughout the same time period as

treatment animals and underwent respiratory challenges at the corresponding time points.

2.3 *Hemorrhage Rabbit Studies*

Hemorrhage studies were conducted in rabbits ($n = 4$) with stepwise (eight steps of 5 mL) removal of a total of 40 mL (~20% blood volume) over 60 min, followed by resuscitation with return of the whole blood by continuous infusion over 60 min (0.66 mL/min). Respiratory challenges, with decreases in inspired O_2 from 100% to 21%, were applied for 5 min three times during hemorrhage and resuscitation phases.

2.4 *CN Rabbit Studies*

For CN rabbit studies ($n = 5$), 10 mg of sodium CN in 60 cc normal saline was infused through the femoral vein at a rate of 1 cc/min (0.167 mg NaCN/min). Respiratory challenges were applied as described above; before, during, and after CN infusion. Changes in hemoglobin concentrations and CcO redox states were monitored continuously with DOS.

2.5 *DOS Measurements in Rabbit Animal Models*

DOS measurements were obtained through a fiber-optic probe with a diode light emitter and the detector at a fixed distance (10 mm) from the source fiber. The probe was placed on the shaved surface of the right inner thigh of the animal for muscle measurements.

The broadband DOS system we constructed combines multi-frequency FDPM with time-independent NIRS to measure bulk tissue absorption and scattering spectra.[26,27,38–41] It employs five laser diodes at discrete wavelengths (660, 685, 786, 822, and 852 nm), and a fiber-coupled avalanche photodiode (APD) detector (Hamamatsu high-speed APD module C5658, Bridgewater, New Jersey) for the frequency domain measurements. Absorption and reduced scattering coefficients are measured directly at each of the five laser diode wavelengths using frequency-dependent phase and amplitude data. Steady-state acquisition was a broadband reflectance measurement from 650 to 1000 nm that follows frequency domain measurements using a tungsten-halogen light source (Ocean Optics HL-2000, Dunedin, Florida) and a spectrometer (BWTEK BTC611E, Newark, Delaware). Intensity of the steady-state reflectance measurements is calibrated to the frequency domain values of absorption and scattering to establish the absolute reflectance intensity.[27,38,39] The acquisition time is ~10 s for the frequency domain measurements and broadband steady-state measurement combined for each measurement.

The key challenges for *in vivo* optical monitoring of CcO redox changes come from the fact that there is a significant overlap in the NIR spectra of hemoglobin and the respiratory chain. Concurrent changes in hemoglobin saturation or volume with CcO redox shift would produce complex spectral changes dominated by hemoglobin due to its high content and high intrinsic absorption. We have made several changes from the previous DOS measurement for CcO redox states changes during CN poisoning.[28] The broadband reflectance measurement was carried out between 650 and 1000 nm focusing on the NIR absorptions centered at 830 nm, which are associated with the Cu_A center.[16] Absorption below 650 nm was excluded from data processing to avoid potential complications from the much stronger absorption changes due to cyt a and cyt a_3 in this region, which could confuse the interpretation of the NIR spectra which are predominantly from Cu_A.[9,32]

At the baseline, broadband reduced scattering coefficients are calculated as a function of wavelength throughout the NIR region (650 to 1000 nm) by fitting a power-law to five discrete frequency domain reduced scattering coefficients and are used throughout the entire data analysis to extract absorption spectra. At each subsequent measurement, the difference absorption spectra are calculated with respect to baseline values. Finally, the changes in chromophore concentrations as well as changes in CcO redox states are calculated from the difference absorption spectra by a linear least squares fit of the wavelength-dependent extinction coefficient spectra of each chromophore in the current approach. We used published absorption spectra for hemoglobins,[42] water,[43] lipid,[44] and difference spectra of CcO (Ref. 45) (downloaded from http://www.ucl.ac.uk/medphys/research/borl/intro/spectra) for the subsequent fitting and analysis.

3 Results

Table 1 presents the baseline chromophore concentration values from DOS measurements in the three rabbit models. Tissue oxyhemoglobin (OxyHb) and deoxyhemoglobin (DeOxyHb) concentrations undergo changes during physiological challenges as shown in the following figures. The water fraction, the water concentration in tissue relative to the concentration of pure water (55.6 M) and the lipid fraction, the lipid mass density ($g\,mL^{-1}$) in tissue relative to a lipid mass density of 0.9 $g\,mL^{-1}$, remain fairly constant. Water and lipid fraction varied less than 4% and 2%, respectively. Table 1 also lists the parameters associated with the power-law fit of five discrete

Table 1 Baseline chromophore concentration values from DOS measurements in the three rabbit models. The water fraction is the water concentration in tissue relative to the concentration of pure water (55.6 M) and the lipid fraction is the lipid mass density ($g\,mL^{-1}$) in tissue relative to a lipid mass density of 0.9 $g\,mL^{-1}$. DeOxyHb, OxyHb, and THb represent deoxyhemoglobin, oxyhemoglobin, and total hemoglobin (OxyHb + DeOxyHb), respectively. Parameters associated with the power-law fit of five discrete frequency domain reduced scattering coefficients at baseline, prefactor (A), and scattering power (SP) where $\mu_s'(\lambda) = A\lambda^{-SP}$, from three rabbit models are also listed. Data are presented as mean ± SEM (standard error of mean). Numbers of animals in control, CN (10 mg), and hemorrhage are 5, 5, and 4, respectively.

	Lipid (%)	Water (%)	DeOxyHb (μM)	OxyHb (μM)	THb (μM)	A	SP
Control	14.3 ± 0.97	85.4 ± 2.74	13.6 ± 1.01	18.7 ± 2.79	32.2 ± 2.02	7170 ± 6660	−1.19 ± 0.16
CN (10 mg)	18.1 ± 3.42	79.5 ± 2.78	11.3 ± 1.44	17.3 ± 1.66	28.6 ± 2.73	2220 ± 2210	−0.98 ± 0.14
Hemorrhage	17.4 ± 2.66	85.8 ± 4.84	10.7 ± 1.35	21.6 ± 0.82	32.3 ± 2.14	11,220 ± 9134	−1.32 ± 0.18

Table 2 Physiological values of control animals ($n = 5$). Mean arterial pressure (mAP), heart rate (HR), and arterial and venous blood gas measurements (PO_2, partial pressure of O_2; BE, base excess; pH) at baseline and 10, 55, and 85 min after the completion of saline infusion are listed. The subscripts a and v designate arterial and venous values, and bpm indicates beats per minute of the heart rate. Data are presented as mean ± SEM. One-way repeated measures analysis of variance (ANOVA) test are performed for physiological parameters presented in this table and the significant mean differences among four time points are reported at the 0.05 significance level.

	Baseline		Post 10 min		Post 55 min		Post 85 min	
	Mean	SEM	Mean	SEM	Mean	SEM	Mean	SEM
P_aO_2 (mm Hg)	607.6	32.7	587.0	28.5	580.6	20.9	602.2	10.8
BE_a (mM)	5.3	2.42*	2.5	1.56	1.8	1.76	0.5	2.25*
P_vO_2 (mm Hg)	49.7	3.40	51.4	3.51	51.7	4.95	50.4	4.16
pH_v	7.47	0.03	7.42	0.04	7.37	0.05	7.37	0.05
BE_v (mM)	6.2	1.78*†	3.4	1.68	1.7	1.76*	1.6	1.90†
mAP (mm Hg)	70.6	5.56*	64.5	5.63	65.5	7.09	56.8	5.95*
HR (bpm)	148.0	5.87	144.2	6.13	141.6	5.68	151.8	8.36

Note: Symbols (* and †) are used to indicate the significant mean difference at the 0.05 level from pairwise comparisons

frequency domain reduced scattering coefficients at a baseline in order to obtain broadband reduced scattering coefficients for subsequent measurement and analysis. The power-law fit coefficients, prefactor (A), and scattering power (SP) [$\mu_s'(\lambda) = A\lambda^{-SP}$] from three rabbit experiments are reported in Table 1.

Tables 2 and 3 list the key physiological values from arterial and venous blood gas analysis of control and CN infused animal groups, respectively. One-way repeated measures analysis of variance test are performed for physiological parameters presented in Tables 2 and 3. At the 0.05 significance level, the significant mean differences between groups are reported. From blood gas analysis data of CN infused animal groups (Table 3), notable changes are observed after CN infusion in arterial and venous base excess values, and mean arterial pressure after CN infusion. The changes in these parameters are indicative of CN toxic effects.[27]

Optical properties from DOS of all 14 animals at baseline are presented in Fig. 1. Figure 1(a) shows the baseline broadband scattering coefficients of frequency domain measurement (mean ± standard deviation) and power-law fit estimated broadband reduced scattering coefficient at baseline (mean, blue line). Absolute broadband absorption spectra (mean± standard deviation) at baseline are shown in Fig. 1(b). Black circles (in every 5 nm), blue line, and red dots represent measured absorption coefficients, DOS fitted absorption coefficients and residuals (measured—DOS fitted absorption coefficient), respectively. Figure 1(c) shows the estimated differential pathlength factor (DPF) of all 14 animals at the baseline (mean± standard deviation) at five discrete wavelengths used for the frequency domain measurements of DOS. DPFs are estimated using the baseline absorption and reduced scattering coefficients and the equation described by Fantini et al.[46] The distance

Table 3 Physiological values of CN infused animals ($n = 5$). Mean arterial pressure (mAP), heart rate (HR), and venous blood gas measurements (PO_2, partial pressure of O_2; BE, base excess; pH) at baseline and 10, 55, and 85 min after the completion of CN infusion are listed. The subscripts a and v designate arterial and venous values, and bpm indicates beats per minute of the heart rate. Data are presented as mean ± SEM. One-way repeated measures ANOVA test are performed for physiological parameters presented in this table and the significant mean differences among four time points are reported at the 0.05 significance level.

	Baseline		Post CN 10 min		Post CN 55 min		Post CN 85 min	
	Mean	SEM	Mean	SEM	Mean	SEM	Mean	SEM
P_aO_2 (mm Hg)	527.9	31.7	581.0	28.1	541.7	32.2	583.4	19.0
BE_a (mM)	4.8	0.66*†	−3.8	1.79*	−2.2	1.40†	−0.4	0.91
P_vO_2 (mm Hg)	51.6	2.78	53.4	2.42	56.0	3.23	58.5	4.16
pH_v	7.41	0.02	7.39	0.04	7.35	0.03	7.36	0.04
BE_v (mM)	5.9	0.58*†	−3.4	1.99‡§	−0.3	1.57*‡	0.7	0.97†§
mAP (mm Hg)	76.5	4.37*†	53.2	2.81	55.9	3.12*	60.1	3.82†
HR (bpm)	136.2	8.22*	159.4	12.06*	153.4	12.90	144.2	11.48

Note: Symbols (*, †, ‡, and §) are used to indicate the significant mean difference at the 0.05 level from pairwise comparisons

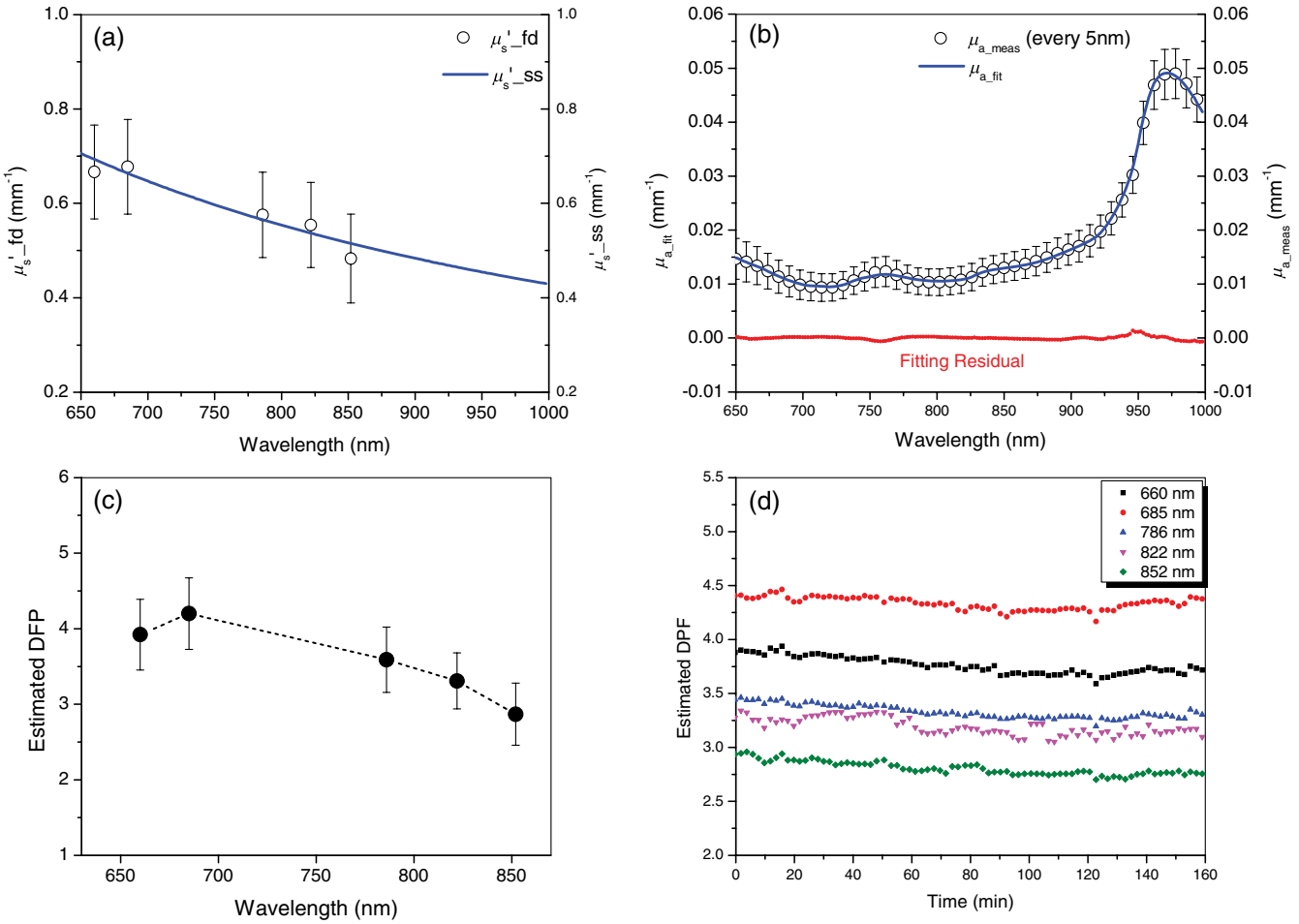

Fig. 1 Optical properties from diffuse optical spectroscopy (DOS) of all 14 animals at the baseline. (a) Baseline broadband scattering coefficients of frequency domain measurement (mean± standard deviation) and power-law fit estimated broadband reduced scattering coefficient at baseline (mean, blue line), (b) absolute broadband absorption spectra (mean ± standard deviation) at baseline are shown. Black circles (in every 5 nm), blue line, and red dots represent measured absorption coefficients, DOS fitted absorption coefficients and residuals (measured—DOS fitted absorption coefficient), respectively. (c) Estimated differential pathlength factor (DPF) of all 14 animals at the baseline (mean ± standard deviation) of five discrete wavelengths used for frequency domain measurements of DOS. DPFs are estimated using the baseline absorption and reduced scattering coefficients and the equation described by Fantini et al. (Ref. 46). The distance between source and detector is 10 mm. (d) Time profile of the estimated DPF of five discrete wavelengths used in DOS measurement. Data are from a single animal in the 10 mg cyanide (CN) group. The distance between the source and detector is 10 mm and the equation described by Fantini et al. is used for the estimation.

between the source and detector is 10 mm. Figure 1(d) shows the time profile of the estimated DPF of five discrete wavelengths used in DOS measurement. Data are from a single animal in the 10 mg CN group.

Figure 2(a) shows the changes in tissue oxy- and deoxyhemoglobin concentrations during hemorrhage and resuscitation in rabbits. In the four hemorrhaged rabbits, tissue OxyHb decreased by 7.47 ± 0.87 μM, and DeOxyHb increased by 3.73 ± 0.99 μM. As a result, tissue hemoglobin oxygen saturation (S_TO_2) decreased by 15.1 ± 4.59%. Also shown in Fig. 2(a) is the time course changes in tissue water fraction of hemorrhage group animals. Although hemorrhage and resuscitation with whole blood has impacted the tissue oxy- and deoxyhemoglobin concentrations and tissue oxygen saturation, the water fraction has stayed steady at the baseline level, which is consistent with the results from our previous study.[47] Figure 2(b) shows the concurrent changes in CcO redox state. The change in CcO redox state parallels the change in OxyHb during hemorrhage and resuscitation: the redox state of CcO becomes increasingly reduced during hemorrhage (-0.69 ± 0.21 μM at the end of hemorrhage) and recovers toward baseline values during whole blood resuscitation (-0.24 ± 0.14 μM at the end of resuscitation). Figure 2 also shows the effect of inspired oxygen concentration challenge during hemorrhage and resuscitation phases. Starting time points of each inspired oxygen challenges are indicated with red arrows. During a reduction in supplemental inspired oxygen respiratory challenge from 100% to 21% O_2, DOS monitoring reveals a decrease in OxyHb and increase in DeOxyHb concentrations. Concurrently, CcO redox state becomes reduced under these challenges.

Figures 3 and 4 demonstrate changes in tissue hemoglobin concentrations and CcO redox state during saline and CN

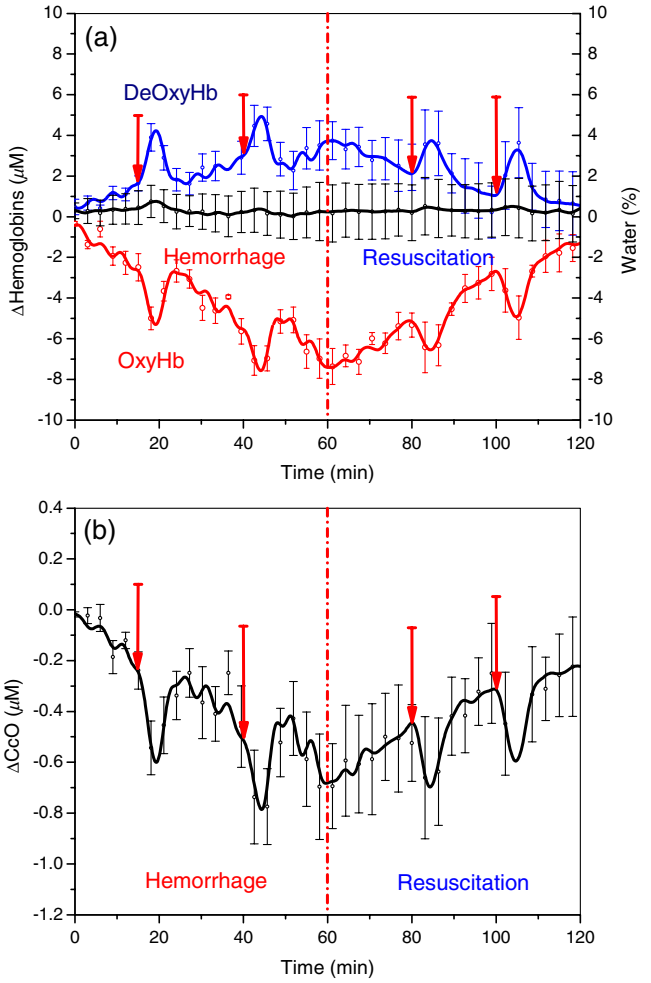

Fig. 2 Changes in tissue oxy- and deoxyhemoglobin (OxyHb, DeOxyHb) concentrations and concurrent changes in CcO redox state during hemorrhage in the rabbit model ($n = 4$). Error bars represent standard error of mean (SEM). Blood volume (40 cc) was removed over 60 min in eight steps via a left femoral artery catheter, and DOS measurements were taken with the probe placed on the right inner thigh muscle. Resuscitation was carried out by continuously infusing autologous blood back to the animal at the rate of 1 mL/ min. Inspired oxygen concentration challenges, where oxygen concentration is decreased briefly from 100% to 21%, were carried out during the hemorrhage and whole blood resuscitation. OxyHb changes parallel changes in CcO redox state during hemorrhage.

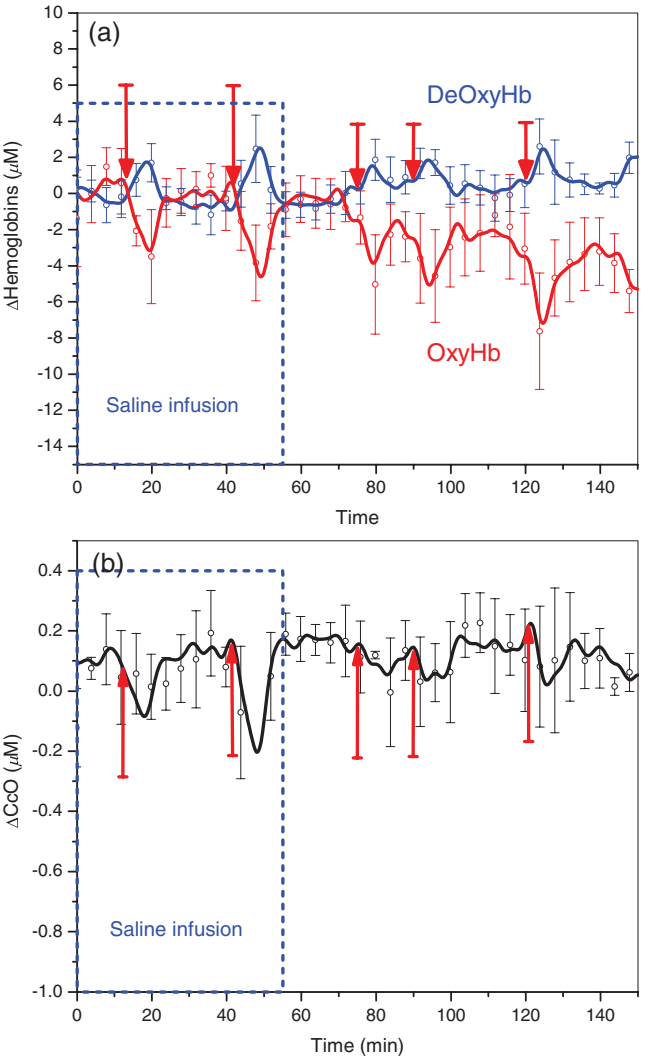

Fig. 3 Changes in hemoglobin concentration and CcO redox state during saline infusion (60 cc) and inspired oxygen concentration challenges in the control animal group ($n = 5$). During saline infusion, no significant change occurs in OxyHb, DeOxyHb, or CcO redox state until the inspired oxygen concentration is decreased briefly from 100% to 21% (F_IO_2 challenges indicated by red arrows). During the F_IO_2 challenges, ΔCcO changes in parallel with changes in OxyHb concentration.

infusion in respective animal models. Saline and NaCN solutions were infused at a rate of 1 cc/ min.

During saline infusion shown in Fig. 3(a), DeOxyHb (blue line) and OxyHb (red line) demonstrate responsiveness to respiratory challenges. DeOxyHb increases during the relative "hypoxic" phase created by reduction of inspired oxygen concentration from 100% to 21%, and returns to baseline values once inspired oxygen concentration is returned back to 100% oxygen. OxyHb responds to respiratory challenges in the opposite direction. CcO redox state in Fig. 3(b) becomes reduced during the relative reduction in inspired oxygen phase and returns to baseline once inspired oxygen concentration is restored to 100%.

Figure 4 shows changes in OxyHb and DeOxyHb concentrations, and CcO redox state responses during CN infusion. In Fig. 4(a), the red curve shows the overall increase in the OxyHb concentration during CN infusion from 0 to 60 min as animals become progressively CN toxic from 0.167 mg NaCN/ min infusion. Conversely, DeOxyHb concentration decreases during CN poisoning due to the inability to extract oxygen from circulating blood in the tissues. Under a "relative" hypoxic respiratory challenge on 21% O_2, continuous DOS monitoring reveals a decrease in OxyHb and increase in DeOxyHb concentrations in CN exposed animals. Concurrently, CcO redox state becomes reduced under these challenges indicated by negative ΔCcO values shown in Fig. 4(b). Combined continuous DOS readings show that OxyHb rises during CN infusion, but drops during respiratory challenges.

This composite effect demonstrates uncoupling of the hemoglobin oxygen signal changes from CcO redox state signals because the CcO redox state becomes reduced with both CN infusion and respiratory challenges, in contrast to the hemoglobin oxygenation state.

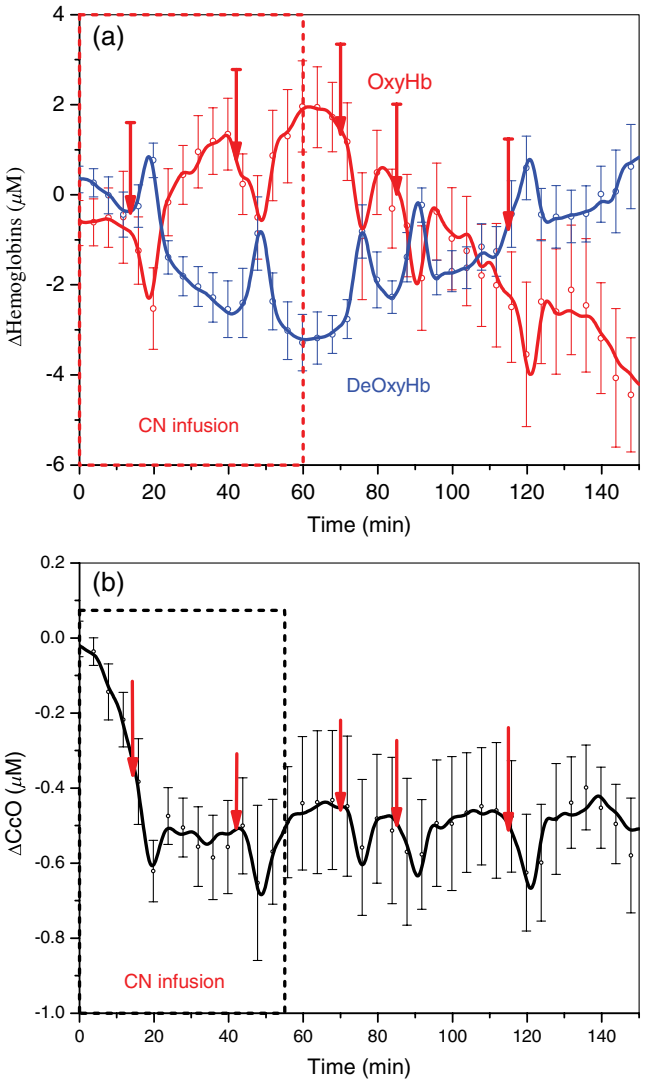

Fig. 4 Changes in hemoglobin concentrations and CcO redox state during CN poisoning and inspired oxygen concentration challenges in 10 mg CN group ($n = 5$). Ten milligrams of sodium CN is infused continuously at a rate of 1 cc/min. Animals receive progressively increasing amount of CN (0.167 mg NaCN/min) for 60 min. (a and b) Changes in OxyHb and DeOxyHb concentrations and ΔCcO changes, respectively. Error bars represent standard error of mean (SEM). During CN infusion, OxyHb changes trend opposite direction of ΔCcO change. However, during F_IO_2 challenges the transient drops in OxyHb are accompanied by similar directional changes in ΔCcO.

Finally, Fig. 5 shows the extracted difference absorption spectra of CcO redox state, DOS fit of difference CcO redox state, and resultant fitting residual after the animal was infused with 8.1 mg of sodium CN, which corresponds to 48.6 min after CN infusion started. From measured difference μ_a spectrum, the absorption contribution from all other chromophores (oxy- and deoxyhemoglobin, water, and lipid) was subtracted to extract absorption signal contributed by changes in the redox state of CcO (black circles). These extracted CcO redox state absorption spectra are compared with DOS fit of CcO redox state changes (blue line). DOS fit of CcO redox state change is the product of the extinction coefficient at each wavelength and the tissue concentration of each animal (-0.62 ± 0.30 μM, mean $\pm$ SD). The extracted difference absorption spectra of CcO redox state

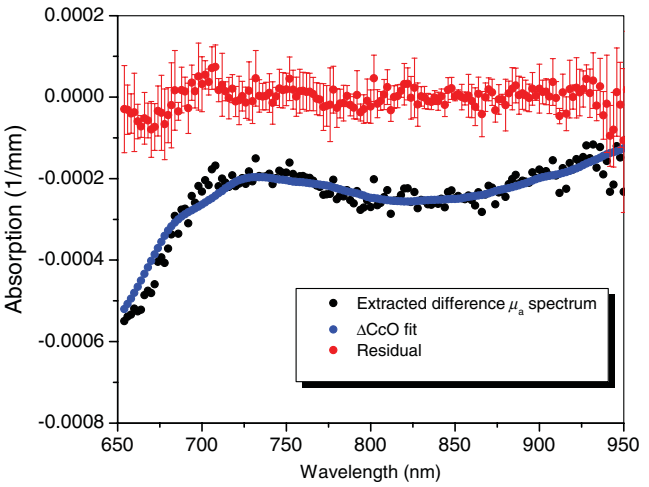

Fig. 5 The extracted difference absorption spectra of CcO redox state (black circles), DOS fit of difference CcO redox state (blue line), and resulting fitting residual (red solid circles) after the animal was infused with 8.1 mg of sodium CN (48.6 min after CN infusion started). Change in ΔCcO is -0.62 ± 0.30 μM from DOS fitting. Mean values of fitting residual (red solid circle) and standard deviation (error bar) are also shown in this figure.

match spectral features and shape of difference CcO μ_a spectrum used for concentration fitting. Red solid circles represent the residual between extracted CcO redox state absorption spectrum and DOS fit from all five animals (mean $\pm$ SD). It is interesting that the residual test of DOS fitting in Fig. 4 shows the spectral features associated with binuclear center ($cyta_3/Cu_B$) at 655 nm as well as the weaker and broad NIR Cu_A band at 830 nm. Figure 5 demonstrates that DOS can measure the changes in CcO redox states in the presence of background chromophore concentration changes in NIR wavelength region between 650 and 1000 nm effectively.

4 Discussion

This study was designed to advance the development of *in vivo* noninvasive optical assessment of CcO redox state. The findings demonstrate that changes in CcO redox state signal can be detected and differentiated from background hemoglobin signal changes under a variety of experimental stress conditions.

As expected, during hemorrhage, the tissue concentration of OxyHb decreases and DeOxyHb increases. During hemorrhage, there is vasoconstriction, reduction in cardiac output and reduction in intravascular total hemoglobin concentration. Since DOS measures the bulk average values of OxyHb, DeOxyHb, and total hemoglobin within the interrogation volume of the tissue, this results in a decrease in the measured total tissue hemoglobin concentration.[24] With the reduction in tissue hemoglobin oxygen delivery to the tissues, increased tissue extraction of oxygen from hemoglobin occurs. All of these factors contribute to a reduction of total oxyhemoglobin content within the tissues measured by DOS; although arterial oxygen saturation is not affected, DOS measures a combination of arterial, capillary, and venous OxyHb, and total quantity of DeOxyHb.[24,25,41,47,48] The tissue DeOxyHb concentration increases due to increased extraction of oxygen from the reduced amount of OxyHb. However, the rise in total tissue DeOxyHb is countered to some degree by vasoconstriction, decreased intravascular hemoglobin, and resultant reduction in total hemoglobin within the tissues. Tissue hemoglobin

saturation (S_TO_2) is calculated as the ratio of OxyHb/total hemoglobin thus falls during hemorrhage.[24,25,41,47,48]

CcO redox state changes parallel to those of OxyHb and S_TO_2 during hemorrhage. As tissue oxygen supply decreases, with hypotension, decreased cardiac output, and anemia, ongoing tissue metabolic oxygen demands continue. This results in a supply:demand imbalance and a decrease of CcO in the oxidized state and an increase of CcO in the reduced state, with an overall reduction in CcO redox state during hemorrhage.

During CN poisoning, OxyHb increases and DeOxyHb decreases due to the inability of tissues to extract oxygen from the blood as a result of inhibition of cytochrome-based electron transport. This results in increased tissue capillary and venous hemoglobin oxygen content as reflected by an increase in OxyHb and decrease in DeOxyHb concentrations with increased tissue hemoglobin oxygen saturation.[28–31]

However, CN poisoning presents a relatively unique situation in which, despite the increase in tissue OxyHb and S_TO_2, the CcO oxidation state decreases. This is a direct result of CN binding and subsequent reduction of the active metal centers in CcO.[14,32,34–36] Thus, during CN poisoning, the direction of change of cytochrome oxidation is opposite to that of hemoglobin oxygenation (unlike that seen during hemorrhage).

During decreases in inspired oxygen concentration, tissue hemoglobin oxygenation decreases. Although arterial hemoglobin is fully oxygen saturated on room air (21% O_2), the partial pressure and oxygen content of dissolved blood oxygen are higher when animals are on 100% inspired oxygen than when on room air. This leads to increases in capillary and venous oxygen content when maintained on 100% inspired oxygen. Thus, as inspired oxygen concentration is decreased from 100% to 21% for brief periods of time, the tissue OxyHb temporarily falls. Although the tissue OxyHb concentration rises during CN poisoning, the CcO redox state moves in the opposite direction, i.e., becomes more reduced. Brief reductions in inspired oxygen from 100% to 21% decrease the tissue OxyHb concentration, and reduce the CcO redox state due to reduction in the quantity and partial pressure of oxygen in the delivered blood. Thus, hemoglobin oxygen saturation and CcO redox states move in the same direction during brief reductions in inspired oxygen, but in opposite directions during continuous CN infusion.

Together, these findings clearly demonstrate uncoupling of OxyHb and DeOxyHb signals from CcO redox signals in peripheral muscle. These findings are further supported by blood gas measurements demonstrating development of acute metabolic acidosis during CN poisoning. Previous *in vitro* studies have shown that anaerobic metabolism commences when approximately 60% of CcO activity has been inhibited by CN.[5] CcO reduction as measured by DOS is an optical measure of redox state, while *in vitro* studies measure CcO enzymatic activity; comparison of the two measures may not be expected to correlate directly.

There are number of limitations of the current study. First, the oxyhemoglobin, deoxyhemoglobin, total hemoglobin, oxidized, and reduced CcO values we report have no gold standard for validation. Thus, while they are consistent with physiologic invasive measurements, the precision and accuracy of the DOS numbers have not been validated. Second, we have clearly demonstrated "uncoupling" of the optical hemoglobin signals from the CcO signals in peripheral muscle. However, whether some underlying degree of partial "cross talk" may affect the CcO redox state remains uncertain. Also third, DOS interrogates a region 2 to 4 mm below the sensor using the source detector separation distances used in these studies. Thus, the ability to extrapolate to deeper events is limited. Additional limitations of this study include the potential contribution of wavelength based spatial variation in tissue signal interrogation in the NIR wavelength range. This could result in deeper tissue region contributions from the higher wavelength regions. The contribution of other cytochrome components cannot be excluded as well. We have attempted to minimize these factors by focusing the analytic spectra above the 650 nm range in this study.

In summary, using unique animal model systems and intervention combinations, these studies demonstrate independence of in vivo DOS CcO redox state measurements from underlying hemoglobin signals in peripheral muscle, where potential interference from myoglobin could occur, unlike in the brain region. Important future directions would include confirmation and correlation of DOS measures of CcO redox state by assessment of anaerobic metabolism based on gas exchange measurements during CN poisoning, and deeper level invasive DOS-based probes for internal organ level assessment. Ultimately, clinical studies will be needed to determine if CcO redox signal measurements can optimize management of tissue CcO redox states in critical disease processes.

Acknowledgments

The authors acknowledge support by the CounterACT Program, Office of the Director, National Institutes of Health (OD) and the National Institute of Environmental Health Sciences (NIEHS), 1U54NS063718, 1U54NS079201, U01-NS058030, U54-NS079201, AMRMC W81XWH-12-2-0114, Air Force FA9550-04-1-0101, FA9550-08-1-0384, and FA9550-10-1-0438; the NIH/NBIB Laser Microbeam and Medical Program P41-EB015890.

References

1. A. H. Hall and B. H. Rumack, "Clinical toxicology of cyanide," *Ann. Emerg. Med.* **15**(9), 1067–1074 (1986).
2. S. I. Baskin and T. G. Brewer, "Medical aspects of chemical and biological warfare. Cyanide poisoning," Chapter 10 in *Textbook of Military Medicine. Part I, Warfare, Weaponry, and the Casualty*, F. R. Sidell et al., Eds., pp. 272–286, Office of the Surgeon General at TMM Publications, Washington, D.C. (1997).
3. T. F. Cummings, "The treatment of cyanide poisoning," *Occup. Med. (Lond.)* **54**(2), 82–85 (2004).
4. G. E. Isom and J. L. Borowitz, "Modification of cyanide toxicodynamics: mechanistic based antidote development," *Toxicol. Lett.* **82–83**, 795–799 (1995).
5. H. B. Leavesley et al., "Interaction of cyanide and nitric oxide with cytochrome c oxidase: implications for acute cyanide toxicity," *Toxicol. Sci.* **101**(1), 101–111 (2008).
6. K. Alexander and S. I. Baskin, "The inhibition of cytochrome oxidase by diaminomaleonitrile," *Biochim. Biophys. Acta* **912**(1), 41–47 (1987).
7. G. T. Babcock and M. Wikstrom, "Oxygen activation and the conservation of energy in cell respiration," *Nature* **356**(6367), 301–309 (1992).
8. J. O. Egekeze and F. W. Oehme, "Cyanides and their toxicity: a literature review," *Tijdschr. Diergeneeskd.* **105**(8, Suppl. 2), 104–114 (1980).
9. F. F. Jobsis et al., "Reflectance spectrophotometry of cytochrome aa3 in vivo," *J. Appl. Physiol.* **43**(5), 858–872 (1977).
10. N. B. Hampson and C. A. Piantadosi, "Near infrared monitoring of human skeletal muscle oxygenation during forearm ischemia," *J. Appl. Physiol.* **64**(6), 2449–2457 (1988).

11. A. D. Edwards et al., "Quantification of concentration changes in neonatal human cerebral oxidized cytochrome oxidase," *J. Appl. Physiol.* **71**(5), 1907–1913 (1991).
12. Y. Hoshi et al., "Redox behavior of cytochrome oxidase in the rat brain measured by near-infrared spectroscopy," *J. Appl. Physiol.* **83**(6), 1842–1848 (1997).
13. T. Noriyuki et al., "Near-infrared spectroscopic method for assessing the tissue oxygenation state of living lung," *Am. J. Respir. Crit. Care Med.* **156**(5), 1656–1661 (1997).
14. C. E. Cooper et al., "Use of mitochondrial inhibitors to demonstrate that cytochrome oxidase near-infrared spectroscopy can measure mitochondrial dysfunction noninvasively in the brain," *J. Cereb. Blood Flow Metab.* **19**(1), 27–38 (1999).
15. C. E. Cooper, D. T. Delpy, and E. M. Nemoto, "The relationship of oxygen delivery to absolute haemoglobin oxygenation and mitochondrial cytochrome oxidase redox state in the adult brain: a near-infrared spectroscopy study," *Biochem. J.* **332**(Pt 3), 627–632 (1998).
16. C. E. Cooper and R. Springett, "Measurement of cytochrome oxidase and mitochondrial energetics by near-infrared spectroscopy," *Philos. Trans. R. Soc., B* **352**(1354), 669–676 (1997).
17. V. Quaresima et al., "Oxidation and reduction of cytochrome oxidase in the neonatal brain observed by in vivo near-infrared spectroscopy," *Biochim. Biophys. Acta* **1366**(3), 291–300 (1998).
18. A. Bainbridge et al., "Brain mitochondrial oxidative metabolism during and after cerebral hypoxia-ischemia studied by simultaneous phosphorus magnetic-resonance and broadband near-infrared spectroscopy," *Neuroimage* (in press) (2013).
19. Y. Sakata et al., "Measurement of the oxidation state of mitochondrial cytochrome c from the neocortex of the mammalian brain," *Biomed. Opt. Express* **3**(8), 1933–1946 (2012).
20. B. Chance and W. Bank, "Genetic disease of mitochondrial function evaluated by NMR and NIR spectroscopy of skeletal tissue," *Biochim. Biophys. Acta* **1271**(1), 7–14 (1995).
21. F. Bevilacqua et al., "Broadband absorption spectroscopy in turbid media by combined frequency-domain and steady-state methods," *Appl. Opt.* **39**(34), 6498–6507 (2000).
22. D. J. Jakubowski, *Development of Broadband Quantitative Tissue Optical Spectroscopy for the Non-Invasive Characterization of Breast Disease, Beckman Laser Institute*, University of California Irvine, Irvine (2002).
23. B. J. Tromberg et al., "Non-invasive in vivo characterization of breast tumors using photon migration spectroscopy," *Neoplasia* **2**(1–2), 26–40 (2000).
24. J. Lee et al., "Hemoglobin measurement patterns during noninvasive diffuse optical spectroscopy monitoring of hypovolemic shock and fluid replacement," *J. Biomed. Opt.* **12**(2), 024001 (2007).
25. J. Lee et al., "Broadband diffuse optical spectroscopy assessment of hemorrhage- and hemoglobin-based blood substitute resuscitation," *J. Biomed. Opt.* **14**(4), 044027 (2009).
26. J. Lee et al., "Noninvasive in vivo monitoring of methemoglobin formation and reduction with broadband diffuse optical spectroscopy," *J. Appl. Physiol.* **100**(2), 615–622 (2006).
27. J. Lee et al., "Non-invasive in vivo diffuse optical spectroscopy monitoring of cyanide poisoning in a rabbit model," *Physiol. Meas.* **28**(9), 1057–1066 (2007).
28. J. Lee et al., "Noninvasive in vivo monitoring of cyanide toxicity and treatment using diffuse optical spectroscopy in a rabbit model," *Mil. Med.* **174**(6), 615–621 (2009).
29. M. Brenner et al., "Sulfanegen sodium treatment in a rabbit model of sub-lethal cyanide toxicity," *Toxicol. Appl. Pharmacol.* **248**(3), 269–276 (2010).
30. M. Brenner et al., "Intramuscular cobinamide sulfite in a rabbit model of sublethal cyanide toxicity," *Ann. Emerg. Med.* **55**(4), 352–363 (2010).
31. M. Brenner et al., "Comparison of cobinamide to hydroxocobalamin in reversing cyanide physiologic effects in rabbits using diffuse optical spectroscopy monitoring," *J. Biomed. Opt.* **15**(1), 017001 (2010).
32. C. A. Piantadosi, A. L. Sylvia, and F. F. Jobsis, "Cyanide-induced cytochrome a, a3 oxidation-reduction responses in rat brain in vivo," *J. Clin. Invest.* **72**(4), 1224–1233 (1983).
33. A. Villringer and B. Chance, "Non-invasive optical spectroscopy and imaging of human brain function," *Trends Neurosci.* **20**(10), 435–442 (1997).
34. H. Beinert et al., "Studies on the origin of the near-infrared (800–900 nm) absorption of cytochrome c oxidase," *Biochim. Biophys. Acta* **591**(2), 458–470 (1980).
35. C. A. Piantadosi and A. L. Sylvia, "Cerebral cytochrome a,a3 inhibition by cyanide in bloodless rats," *Toxicology* **33**(1), 67–79 (1984).
36. M. Tamura, "Protective effects of a PGI2 analogue OP-2507 on hemorrhagic shock in rats—with an evaluation of the metabolic recovery using near-infrared optical monitoring," *Jpn. Circ. J.* **56**(4), 366–375 (1992).
37. C. E. Cooper et al., "Measurement of cytochrome oxidase redox state by near infrared spectroscopy," *Adv. Exp. Med. Biol.* **413**, 63–73 (1997).
38. F. Bevilacqua et al., "Broadband absorption spectroscopy in turbid media by combined frequency-domain and steady-state methods," *Appl. Opt.* **39**(34), 6498–6507 (2000).
39. T. H. Pham et al., "Broad bandwidth frequency domain instrument for quantitative tissue optical spectroscopy," *Rev. Sci. Instrum.* **71**(6), 2500–2513 (2000).
40. S. Merritt et al., "Comparison of water and lipid content measurements using diffuse optical spectroscopy and MRI in emulsion phantoms," *Technol. Cancer Res. Treat.* **2**(6), 563–569 (2003).
41. J. Lee et al., "Broadband diffuse optical spectroscopy measurement of hemoglobin concentration during hypovolemia in rabbits," *Physiol. Meas.* **27**(8), 757–767 (2006).
42. W. G. Zijlstra, A. Buursma, and O. W. Assendelft, *Visible and Near-infrared Absorption Spectra of Human and Animal Hemoglobin*, VSP BV, AH Zeist, Netherlands (2000).
43. L. H. Kou, D. Labrie, and P. Chylek, "Refractive indices of water and ice in the 0.65 to 2.5 mm spectral range," *Appl. Opt.* **32**(19), 3531–3540 (1993).
44. C. Eker, "*Optical Characterization of Tissue for Medical Diagnostics*," Lund University, Lund, Sweden (1999).
45. S. Wray et al., "Characterization of the near infrared absorption spectra of cytochrome aa3 and haemoglobin for the non-invasive monitoring of cerebral oxygenation," *Biochim. Biophys. Acta* **933**(1), 184–192 (1988).
46. S. Fantini et al., "Non-invasive optical monitoring of the newborn piglet brain using continuous-wave and frequency-domain spectroscopy," *Phys. Med. Biol.* **44**(6), 1543–1563 (1999).
47. J. Lee et al., "Tissue hemoglobin monitoring of progressive central hypovolemia in humans using broadband diffuse optical spectroscopy," *J. Biomed. Opt.* **13**(6), 064027 (2008).
48. T. H. Pham et al., "Noninvasive monitoring of hemodynamic stress using quantitative near-infrared frequency-domain photon migration spectroscopy," *J. Biomed. Opt.* **7**(1), 34–44 (2002).

Biographies of the authors are not available.